

Density functional theory in transition-metal chemistry: a self-consistent Hubbard U approach

Heather J. Kulik, Matteo Cococcioni, Damian A. Scherlis, and Nicola Marzari

Department of Materials Science and Engineering,
Massachusetts Institute of Technology, Cambridge, MA 02139, USA
(dated: June 6, 2021)

Transition-metal centers are the active sites for many biological and inorganic chemical reactions. Notwithstanding this central importance, density-functional theory calculations based on generalized-gradient approximations often fail to describe energetics, multiplet structures, reaction barriers, and geometries around the active sites. We suggest here an alternative approach, derived from the Hubbard U correction to solid-state problems, that provides an excellent agreement with correlated-electron quantum chemistry calculations in test cases that range from the ground state of Fe_2 and Fe_2^+ to the addition-elimination of molecular hydrogen on FeO^+ . The Hubbard U is determined with a novel self-consistent procedure based on a linear-response approach.

Transition metals are central to our understanding of many fundamental reactions, as active sites in naturally-existing or synthetic molecules that range from metalloporphyrins and oxidoreductases [1] to alkene metathesis catalysts [2] to light-harvesting photosynthetic complexes [3]. Despite this relevance, most electronic-structure approaches fail to describe consistently or accurately transition-metal centers. Examples include neutral and charged iron dimers [4], FeO^+ [5], Mn(salen) epoxidation catalysts [6], or hemeproteins [7].

In this Letter, we argue that generalized gradient approximations (GGA) [8] augmented by a Hubbard U term [9], already very successful in the solid state [10, 11], also greatly improve single-site or few-site energies, thanks to a more accurate description of self- and intra-atomic interactions. Nevertheless, U is not a fitting parameter, but an intrinsic response property: as shown by Cococcioni and de Gironcoli [12], U measures the spurious curvature of the GGA energy functional as a function of occupations, and GGA+U largely recovers the piecewise-linear behavior of the exact ground-state energy. U is determined by the difference between the screened and bare second derivative of the energy with respect to on-site occupations $\frac{\partial^2 E}{\partial n_i^2} = \frac{\partial^2 E}{\partial n_i^2} - \frac{\partial^2 E}{\partial n_i^2}$ (i is the spin-orbital, and I the atomic site) [12]. While in the original derivation U was calculated from the GGA ground state, we argue here that U should be consistently obtained from the GGA+U ground state itself. This becomes especially relevant when GGA and GGA+U differ qualitatively (metal vs. insulator in the solid state, different symmetry in a molecule). To clarify our approach, we first identify in the GGA+U functional the electronic terms that have quadratic dependence on the occupations:

$$E_{\text{quad}} = \frac{U_{\text{scf}}}{2} \sum_{I,i} \sum_{J,j} X_{I,i} X_{J,j} + \frac{U_{\text{in}}}{2} \sum_{I,i} X_{I,i}^2 \quad (1)$$

The first term represents the contribution already contained in the standard GGA functional, modeled here as a double-counting term, while the second term is the customary $+U$ correction. Therefore, U_{scf} represents the effective on-site electron-electron interaction already present in the GGA energy functional for the GGA+U ground state when U is chosen to be U_{in} . Consistency is enforced by choosing U_{in} to be equal to U_{scf} . The U_{scf} obtained from linear-response [12] (labeled here U_{out}) is also obtained by differentiating Eq. 1 with respect to $\frac{\partial E}{\partial n_i}$:

$$U_{\text{out}} = \frac{d^2 E_{\text{quad}}}{d(\frac{\partial E}{\partial n_i})^2} = U_{\text{scf}} \frac{U_{\text{in}}}{m}; \quad (2)$$

where $m = \sum_i \sum_I (a_{I,i}^I)^2$ can be interpreted as an effective degeneracy of the orbitals whose population is changing during the perturbation (to linear order, $\frac{\partial n_i}{\partial U_{\text{in}}} = a_{I,i}^I \frac{\partial a_{I,i}^I}{\partial U_{\text{in}}}$ with $\sum_i a_{I,i}^I = 1$ and $\frac{d^2}{d(\frac{\partial E}{\partial n_i})^2} = \sum_{ij} a_{I,i}^I a_{I,j}^I \frac{d^2}{d(\frac{\partial E}{\partial n_i})^2}$). Even if in principle U_{scf} depends on U_{in} , we find it to be constant over a broad interval, as apparent from Fig. 1: U_{out} is linear in U_{in} for the relevant range of $U_{\text{in}} - U_{\text{scf}}$. Thus, from few linear-response calculations for different U_{in} ground states we are able to extract the U_{scf} that should be used.

We employ this formulation in the study of the Fe_2 and Fe_2^+ dimers and the addition-elimination reaction of molecular hydrogen on FeO^+ : these are paradigmatic cases of the challenges for first-principles methods to accurately reproduce the many low-lying multiplet potential energy surfaces associated with transition metals. It has been argued that spin density functional theory can describe the lowest lying state of a given spatial and spin symmetry [13, 14], but difficulties remain in obtaining accurate multiplet splittings [15]. Our GGA or GGA+U calculations have been performed with Quantum-ESPRESSO [16]; coupled cluster (CCSD(T)) and B3LYP calculations have been performed with Gaussian03 [18].

The iron dimer has been investigated both theoretically [4, 19, 20, 21] and experimentally [22, 23, 24].

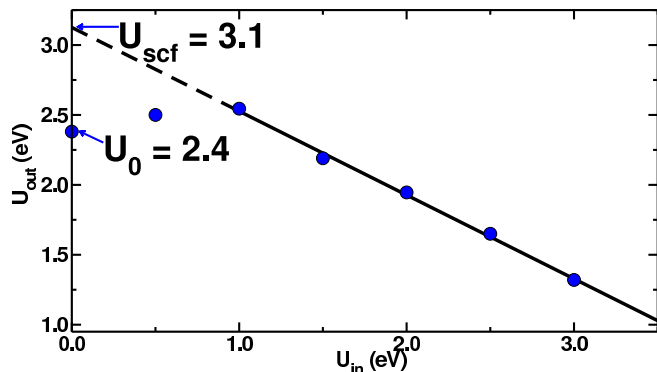


FIG. 1: Linear-response U_{out} calculated from the GGA + U_{in} ground state of ${}^7_u \text{Fe}_2$, together with the extrapolated U_{scf} . U_0 is U_{out} calculated for $U_{\text{in}} = 0$.

The experimental photoelectron spectrum of Fe_2 below 2 eV is remarkably simple – there are only two prominent peaks, one at 1.0 eV and a second peak 0.53 eV above it, corresponding to two allowed transitions to different neutral Fe_2 states [23]. A recent multi-reference configuration-interaction (MRCI) study [20] has assigned the three experimental electronic states involved as 8_u for Fe_2 and 9_g and 7_g for Fe_2 ; more recently, CCSD(T) has been shown to be in overall agreement [21]. Importantly, these electronic states are consistent with the experimental measurements for the anion (fundamental frequency $\nu_0 = 250 \pm 20 \text{ cm}^{-1}$ and bond length $R_e = 2.10 \pm 0.04 \text{ \AA}$), and the two neutral Fe_2 states, which display similar properties ($\nu_0 = 300 \pm 15 \text{ cm}^{-1}$ and $R_e = 2.02 \pm 0.02 \text{ \AA}$) [23].

We first apply our approach to Fe_2 and Fe_2^- . We obtain a U_0 of 2 eV (i.e. when calculated from the GGA ground state) and a U_{scf} of 3 eV (since energies at different U are not directly comparable, we average U_0 and U_{scf} over all states considered). GGA + U_{scf} shows a striking and consistent agreement with MRCI [20] and our CCSD(T) results, correctly identifying both the lowest anion state 8_u ($3d: \begin{smallmatrix} 2 & 4 & 2 \\ g & u & g \end{smallmatrix} i^2 \begin{smallmatrix} 2 & 2 \\ u & u \end{smallmatrix} i^1 4s: \begin{smallmatrix} 2 \\ g & u \end{smallmatrix} i^2$) and the first excited state, 8_g , 0.38 eV above. The lowest, singly ionized neutral states, which differ from Fe_2 only by the loss of the spin down or spin up ($4s$) orbital, are 9_g and 7_g . The 9_g / 7_g GGA + U_{scf} splitting of 0.6 eV compares very well with theoretical results (MRCI and CCSD(T)) and the experimental splitting (0.53 eV) in Table I. The structure of these two states (see Table II) is also consistent with experimentally observed close similarity of R_e and ν_0 for the two neutral states and the modest decrease in R_e (0.08 \AA) and increase in ν_0 (50 cm^{-1}) with respect to Fe_2 [23].

In stark contrast with MRCI, CCSD(T) and GGA + U_{scf} , GGA favors the 8_g Fe_2 state ($3d^{14}: \begin{smallmatrix} 2 & 4 & 3 \\ g & u & g \end{smallmatrix} i^2 \begin{smallmatrix} 2 & 2 \\ u & u \end{smallmatrix} i^1, 4s^3: \begin{smallmatrix} 2 \\ g & u \end{smallmatrix}$) by as much as 0.9 eV relative to other methods. Neutral states arising from single ionization of the 8_g state are 7_u ($3d^{14} 4s^2$) and 9_g

State	B3LYP	GGA	+ U_0 (2eV)	+ U_{scf} (3eV)	CCSD (T)	MRCI ^a
8_g	0.00	0.00	0.00	0.00	0.00	0.00
8_g	0.14	-0.52	0.04	0.38	0.40	0.45
9_g	0.00	0.00	0.00	0.00	0.00	0.00
7_g	0.34	0.65	0.66	0.60	0.55	0.62
7_u	0.18	-0.12	0.48	0.72	0.86	0.69
9_g	0.36	0.28	0.36	0.41	0.38	0.45

TABLE I: Multiplet splittings (in eV) for Fe_2^- and Fe_2 at several levels of theory. (a) Ref. [20].

State	GGA	GGA + U_{scf}	CCSD (T)	MRCI ^a	Expt. ^b
8_g	2.20, 305	2.20, 301	2.24, 276	2.23, 272	2.1, 250
8_g	2.07, 360	2.08, 355	2.12, 321	2.4, {	{
9_g	2.11, 339	2.13, 335	2.17, 296	2.18, 299	2.0, 300
7_g	2.10, 335	2.12, 331	2.16, 304	2.17, 310	2.0, 300
7_u	1.99, 413	2.00, 419	2.00, 404	2.25, 195	{
9_g	2.26, 285	2.26, 280	2.28, 220	2.35, {	{

TABLE II: Bond lengths (\AA) and harmonic frequencies, ν_e , (cm^{-1}) for Fe_2^- and Fe_2 , compared to experiment (here, fundamental frequencies, ν_0). (a) Ref. [20]. (b) Ref. [23].

($3d^{13} 4s^3$) which result from the loss of ${}^u(4s)$ and ${}^g(3d)$ electrons, respectively. In addition, these two states have differing bond lengths (R_e of 1.99 and 2.26 \AA) and frequencies (ν_e of 413 cm^{-1} and 285 cm^{-1}), and thus are not compatible with experiment [4, 23].

Our second test case explores the potential energy surfaces of the highly exothermic ($\Delta H < -1.6 \text{ eV}$) addition-elimination reaction of molecular hydrogen on bare FeO^+ . This spin-allowed reaction occurs with exceedingly low efficiency (1 in every 100-1000 gas-phase collisions results in products), yet when it does proceed it is observed to be barrierless [25, 26, 27]. This apparent contradiction has been explained by a two-state-reactivity model [5, 28, 29], wherein the steep reaction barriers along the spin surface of the reactants and products (sextets in both cases) preclude an efficient, exothermic reaction. Instead, the reaction must occur along a shallow but excited spin surface (here, the quartet), and the reaction bottleneck is the coupling of the two surfaces which permits the necessary spin-inversion at the entrance and exit channels. For several exchange-correlation functionals, (including B3LYP) [5, 29], the reaction coordinates have failed to agree qualitatively with experiments [25, 26, 27], higher level correlated-electron calculations [28, 30], or with the established paradigm of a two-state model [29].

For the bare FeO^+ reactant, GGA predicts a ${}^6+$ ground state and two nearly degenerate low-lying quartet states, 4 and 4 , 0.84 eV above. GGA + U_{scf} (5.5 eV) preferentially stabilizes 4 FeO^+ and yields a ${}^6+$ / 4

M ethod	${}^6\text{FeO}^+$			${}^4\text{FeO}^+$		
	R_e	ν_e	$\nu_e x_e$	R_e	ν_e	$\nu_e x_e$
GGA	1.62	901	328	1.56	1038	332
GGA+U	1.66	749	432	1.75	612	172
CCSD(T)	1.66	724	434	1.70	633	188

TABLE III: Equilibrium bond lengths, R_e (Å), harmonic frequencies, ν_e (cm^{-1}), and anharmonicity, $\nu_e x_e$ (cm^{-1}) for the 6 and 4 states of FeO^+ .

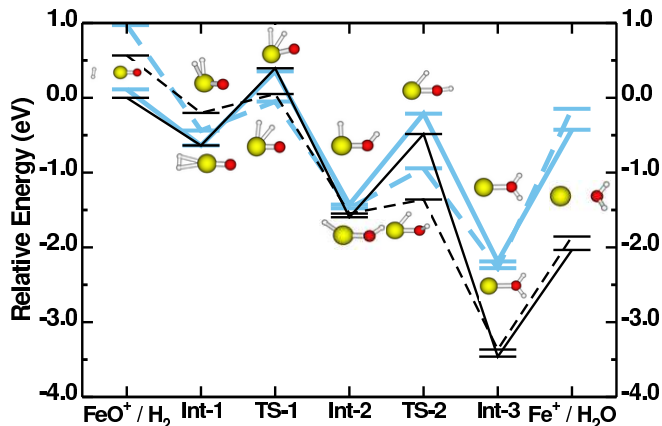


FIG. 2: Potential energy surface and geometries for the $\text{FeO}^+ + \text{H}_2$ reaction using GGA (blue) as compared against a CCSD(T) reference (black). Solid indicates sextet while dashed indicates quartet. (Color online.)

splitting of 0.54 eV in quantitative agreement with the symmetry and splitting (0.57 eV) predicted by CCSD(T). The U correction also reduces the 3d character of minority spin molecular orbitals which dramatically improves bond lengths, harmonic frequencies, and anharmonicity, as shown in Table III.

We thus proceed to study the full sextet and quartet potential energy surfaces (PES) for this reaction. We stress that, as is commonly found for open-shell transition-metal molecules, several low-lying PES exist for each multiplicity and we present results for the lowest-lying symmetry of each multiplicity. The U_{scf} applied in this global PES is 5 eV, very close to the average of the U_{scf} (4.93 eV) calculated for the quartet (5.02 eV) and sextet (4.84 eV) at each stationary point; the values of U_0 are similar (quartet = 4.71 eV; sextet = 4.76 eV). Although most states possess a U_{scf} close to the global average, the few deviations will be highlighted later.

Our GGA results for the intermediates (Int) and transition states (TS) along the reaction coordinate confirm the previously noted failures. Aside from the overestimate of FeO^+ splittings, the most notable deviations are unusually steep barriers (0.54 eV) along the quartet surface, lack of spin-crossing near the products, and a dramatic underestimate in the exothermicity, as depicted in Fig. 2 [33].

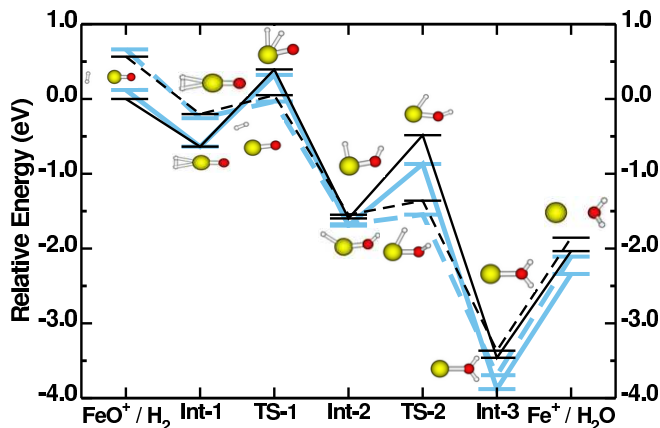


FIG. 3: Potential energy surface and geometries for the $\text{FeO}^+ + \text{H}_2$ reaction using GGA+U (5 eV) (blue) as compared against a CCSD(T) reference (black). Solid indicates sextet while dashed indicates quartet, as in Fig. 2. (Color online.)

$E_{6:4}$	GGA	GGA+U	CCSD(T)
FeO^+	0.84	0.54	0.57
Int-1	0.20	0.38	0.43
Int-2	-0.05	0.03	0.05
Int-3	-0.09	0.19(0.12)	0.09
Fe^+	0.25	0.22	0.18

TABLE IV: Multiplet splittings (in eV) using GGA, GGA+U (U = 5 eV except in parentheses, $U_{\text{Int } 3;\text{av}} = 3.5$ eV) and CCSD(T).

With GGA+U (5 eV), we obtain consistency with CCSD(T), as shown in Fig. 3. The reactant FeO^+ splitting is reduced, the splitting at Int-1 increases, corresponding to a shallow quartet reaction coordinate, and the exothermicity and spin crossover near the products are in good agreement with experiment and theoretical paradigm [5]. The quantitative accuracy of GGA+U becomes fully evident in the intermediate splittings (Table IV), forward and back reaction barriers (Table V), and overall mean absolute errors (MAE) in multiplet splittings that are reduced (with respect to CCSD(T) reference) from 0.20 eV for GGA to 0.04 eV for GGA+U. Geometries are also improved: the MAE for bond lengths

E_a	Forward Reaction			Back Reaction		
	GGA	GGA+U	CCSD(T)	GGA	GGA+U	CCSD(T)
TS-1 ⁴	0.39	0.22	0.25	1.43	1.64	1.60
TS-1 ⁶	0.99	0.96	1.03	1.60	2.02	1.99
TS-2 ⁴	0.54	0.13	0.19	1.34	2.15	2.01
TS-2 ⁶	1.22	0.82(1.16)	1.11	2.01	3.01	2.98

TABLE V: Comparison of GGA, GGA+U (U = 5 eV except in parentheses, $U_{4s} = U_{3d} = 4$ eV) and CCSD(T) forward and back reaction barriers (in eV).

are reduced from 4.3 pm (GGA) to 2.2 pm (GGA+U). [34]. The GGA+U and CCSD(T) states also possess consistent orbital occupations and symmetry.

The few examples of U_{scf} deviating from 5 eV are primarily at the exit channel, where large changes in hybridization occur. The quartet Int-3 is the only case for which we obtain a low U_{scf} (2 eV) which originates from the reduced hybridization of Fe 3d states. We chose to recalculate the splitting with a $U_{scf;av}$ that was a local average on the Int-3 states. With this U of 3.5 eV, we obtain a splitting of 0.12 eV, in even closer agreement with CCSD(T). While this reduced hybridization of the 3d states is unusual, we stress that it is consistently predicted in our linear-response approach. Along the sextet surface, the iron valence occupations correspond to $3d^6 4s^1$, and we find that the interplay of 3d and 4s states to be critical for describing the second barrier along the sextet reaction surface. A matrix extension of our formalism [12] considers also the response of the 4s orbitals, and we obtain $U_{4s;scf} = 4.0$ eV and $U_{3d;scf} = 4.0$ eV around the barrier (U_{4s} is instead found to be nearly zero elsewhere). Inclusion of the 4s response for both sextets Int-2 and Int-3 increases the forward reaction barrier to 1.16 eV while the backward barrier remains unchanged – in accordance with CCSD(T).

In conclusion, we have shown how a self-consistent GGA+U approach can provide a dramatic improvement to the description of multiplet potential energy surfaces for transition-metal complexes that are otherwise poorly described by common exchange-correlation functionals, while preserving the very favorable computational costs and scaling of local density-based functionals. These improvements include spin energetics, state symmetries, and quantitative description of complex reaction coordinates. U has been treated as an intrinsic, non-empirical property of the system considered, and never as a fitting parameter, and it has been obtained through a self-consistent extension to the linear-response formulation of Cococcioni and de Gironcoli [12]. Such development will allow large-scale and accurate calculations [31] on transition-metal complexes, with applications in the field of catalysis, biochemistry, and environmental science.

We thank F. de Angelis for pointing out the H_2 on FeO^+ reaction and S. de Gironcoli for helpful discussions on U_{scf} . This work was supported by an NSF graduate fellowship and ARO-MURIDAAD-19-03-1-0169. Computational facilities were provided through NSF grant DMR-0414849 and PNNL grant EM-SL-UP-9597.

Current Address: Departamento de Química Inorgánica, Analítica y Química Física, Universidad de Buenos Aires

[1] A. C. Rosenzweig et al., *Nature* 366, 537 (1993).

[2] R. R. Schrock and J. A. Osborn, *J. Am. Chem. Soc.* 98, 2134 (1976).

[3] P. Jordan et al., *Nature* 411, 909 (2001).

[4] D. G. Leopold et al., *J. Chem. Phys.* 88, 3780 (1988).

[5] S. Shaik and M. Filatov, *J. Phys. Chem. A* 102, 3835 (1998).

[6] L. Cavallo and H. Jacobsen, *J. Phys. Chem. A* 107, 5466 (2003).

[7] C. Rovira et al., *Biophys. J.* 81, 435 (2001).

[8] J. P. Perdew, K. Burke, and M. Ernzerhof, *Phys. Rev. Lett.* 77, 3865 (1996).

[9] V. I. Anisimov, J. Zaanen, and O. K. Andersen, *Phys. Rev. B* 44 943 (1991).

[10] F. Zhou et al., *Phys. Rev. B* 70, 235121 (2004).

[11] A. I. Liechtenstein, V. I. Anisimov, and J. Zaanen *Phys. Rev. B* 52, R5467 (1995).

[12] M. Cococcioni and S. de Gironcoli, *Phys. Rev. B* 71, 035105 (2005).

[13] T. Ziegler, A. Rauk and E. J. Baerends, *Theor. Chim. Acta.* 43, 261 (1977).

[14] O. Gunnarsson and B. I. Lundqvist, *Phys. Rev. B* 13, 4274 (1976); U. von Barth, *Phys. Rev. A* 20, 1693 (1979).

[15] Multiplets are defined by their spin component along the z-axis and are thus not eigenstates of the square of the spin operator. Consequences and alternatives are discussed more fully in M. Filatov and S. Shaik, *J. Chem. Phys.* 110, 116 (1999) and references therein.

[16] S. Baroni et al., <http://www.quantum-espresso.org>. Calculations are completed in the Perdew Burke Ernzerhof (GGA) approximation [8] using ultrasoft pseudopotentials with a plane wave cutoff of 40 Ry and density cutoff of 480 Ry; transition states are obtained with the nudged elastic band method [17].

[17] G. Henkelman, B. P. Uberuaga, and H. Jonsson, *J. Chem. Phys.* 113, 9901 (2000).

[18] M. J. Frisch et al., Gaussian, Inc. (2004). Hybrid functional B3LYP (Becke's 3-parameter exchange and Lee, Yang, and Parr's correlation) and CCSD(T) calculations use the 6-311++G(3df,3pd) basis set.

[19] S. Dhar and N. R. Kestner, *Phys. Rev. A* 38, 1111 (1988).

[20] O. Hubner and J. Sauer, *Chem. Phys. Lett.* 358, 442 (2002) and references therein.

[21] A. Irigoras et al., *Chem. Phys. Lett.* 376, 310 (2003).

[22] T. McNab, H. Micklitz, and P. Barrett, *Phys. Rev. B* 4, 3787 (1971).

[23] D. Leopold and W. Lineberger, *J. Chem. Phys.* 85, 51 (1986).

[24] E. A. Rohlfing et al., *J. Chem. Phys.* 81, 3846 (1984).

[25] D. E. Clemmer et al., *J. Phys. Chem.* 98, 6522 (1994).

[26] D. Schroeder et al., *Int. J. Mass. Spec.* 161, 175 (1997).

[27] J. M. Mercero et al., *Int. J. Mass. Spec.* 240, 37 (2005) and references therein.

[28] A. Fiedler et al., *J. Am. Chem. Soc.* 116, 10734 (1994).

[29] D. Danovich and S. Shaik, *J. Am. Chem. Soc.* 119, 1773 (1997).

[30] A. Irigoras, J. Fowler, and J. Ugalde, *J. Am. Chem. Soc.* 121, 8549 (1999).

[31] P. Giannozzi, F. De Angelis, and R. Car, *J. Chem. Phys.* 120, 5903 (2004).

[32] The ϵ_0 are obtained with a power law following Hollas, *High Resolution Spectroscopy*, Wiley, 1998. Anhamonicity prevents direct comparison to the experimental ϵ_0 .

[33] The PES of Figs. 2 and 3 have been aligned at 6 Int-1.

[34] CCSD(T) geometries are from an 0.01 Å interpolation in each degree of freedom (up to v_e) in total as much as

800 for a structure. The states considered are reactants and intermediates for each quartet and sextet PES.